

DISCOVERY OF THREE PULSATING, MIXED-ATMOSPHERE, EXTREMELY LOW-MASS
WHITE DWARF PRECURSORS*A. GIANNINAS¹, BRANDON CURD¹, G. FONTAINE², WARREN R. BROWN³, AND MUKREMIN KILIC¹,¹Homer L. Dodge Department of Physics and Astronomy, University of Oklahoma, 440 W. Brooks St., Norman, OK 73019, USA; alexg@nhn.ou.edu²Département de Physique, Université de Montréal, C.P. 1628, Succursale Centre-Ville, Montréal, QC, H3C 3J7, Canada and³Smithsonian Astrophysical Observatory, 60 Garden St., Cambridge, MA 02138, USA*Published in ApJ Letters*

ABSTRACT

We report the discovery of pulsations in three mixed-atmosphere, extremely low-mass white dwarf (ELM WD, $M \leq 0.3 M_{\odot}$) precursors. Following the recent discoveries of pulsations in both ELM and pre-ELM WDs, we targeted pre-ELM WDs with mixed H/He atmospheres with high-speed photometry. We find significant optical variability in all three observed targets with periods in the range 320–590 s, consistent in time-scale with theoretical predictions of p -mode pulsations in mixed-atmosphere $\approx 0.18 M_{\odot}$ He-core pre-ELM WDs. This represents the first empirical evidence that pulsations in pre-ELM WDs can only occur if a significant amount of He is present in the atmosphere. Future, more extensive, timeseries photometry of the brightest of the three new pulsators offers an excellent opportunity to constrain the thickness of the surface H layer, which regulates the cooling timescales for ELM WDs.

Keywords: asteroseismology — binaries: close — stars: individual (SDSS J075610.71+670424.7, SDSS J114155.56+385003.0, SDSS J115734.46+054645.6) — techniques: photometric — white dwarfs

1. MOTIVATION

Pulsating white dwarf (WD) stars provide a unique opportunity to probe their internal structure by comparing the observed spectrum of pulsation periods with the predictions of detailed asteroseismic models. Several different families of pulsating WDs are known and they all occupy fairly well defined instability regions in the $T_{\text{eff}}\text{--}\log g$ plane (Fontaine & Brassard 2008; Winget & Kepler 2008). The largest class of pulsating WDs are the so-called ZZ Ceti (or DAV) stars which are found in a narrow range of effective temperature with $11,000 \lesssim T_{\text{eff}} \lesssim 12,500$ K (Gianninas et al. 2011). As these WDs cool and enter the instability strip, they become unstable to non-radial g -mode oscillations driven by a hydrogen partial ionization zone.

Recently, the discovery of pulsations in several extremely low-mass (ELM) WDs has demonstrated that the canonical ZZ Ceti instability strip extends to considerably lower surface gravities ($5 < \log g < 7$) (Hermes et al. 2013a). The ongoing ELM Survey (see Gianninas et al. 2015; Brown et al. 2016, and references therein), has led to the identification of seven pulsating ELM WDs (Hermes et al. 2012, 2013b,a; Bell et al. 2015) including the unique system PSR J1738+0333 (Kilic et al. 2015). These empirical results have been complimented by the theoretical work of Van Grootel et al. (2013), Córscico & Althaus (2014, 2016), and Jeffery & Saio (2016).

Recently, a pair of pulsating stars with evolutionary ties to ELM WDs was discovered. The class of EL CVn-type binaries outlined in Maxted et al. (2014b) are considered to be pre-

cursors to ELM WD systems. The pre-ELM WDs in the EL CVn-type systems WASP J2047–25B and WASP J1628+10B have been shown to pulsate (Maxted et al. 2013, 2014a). These pre-ELM WDs are located outside the boundaries of the extended ZZ Ceti instability strip and thus their pulsations cannot be explained by the usual driving mechanism ascribed to partially ionized hydrogen. Instead, Jeffery & Saio (2013) require significant amounts of helium in the driving region to explain the observed p -mode pulsations in these stars.

Van Grootel et al. (2015) have shown that between the ZZ Ceti instability and the V777 Her instability strip for helium atmosphere WDs, a continuum of instability strips exist as the composition of the atmosphere is varied from pure H to pure He. This phenomenon has recently been explored in greater detail for the ELM WD regime by Córscico et al. (2016).

The discovery of the pulsators in the two WASP systems and the predictions of mixed-atmosphere pulsators outside the confines of the traditional instability strips, spurred us to take a closer look at objects from the ELM Survey where the presence of He in the atmosphere had clearly been detected. In all, six candidates were considered. These include J0751–0141, J1141+3850, J1157+0546, J1238+1946, J1625+3632 (Gianninas et al. 2014b), and J0756+6704 (Gianninas et al. 2015). In Section 2 we describe the pulsation models for these candidates and in Section 3 we present our timeseries photometric observations. In Section 4, we discuss each of the newly discovered pulsators individually and we conclude in Section 5 by discussing the implications of these new discoveries and we consider future avenues of research.

2. PULSATION MODELS

We carried out exploratory stability calculations with the help of the Montréal pulsation codes (Brassard et al. 1992; Fontaine et al. 1994). The equilibrium models that we constructed are envelope models – entirely suitable for investi-

* Based on observations obtained at the Gemini Observatory, which is operated by the Association of Universities for Research in Astronomy, Inc., under a cooperative agreement with the NSF on behalf of the Gemini partnership: the National Science Foundation (United States), the National Research Council (Canada), CONICYT (Chile), Ministerio de Ciencia, Tecnología e Innovación Productiva (Argentina), and Ministério da Ciência, Tecnologia e Inovação (Brazil).

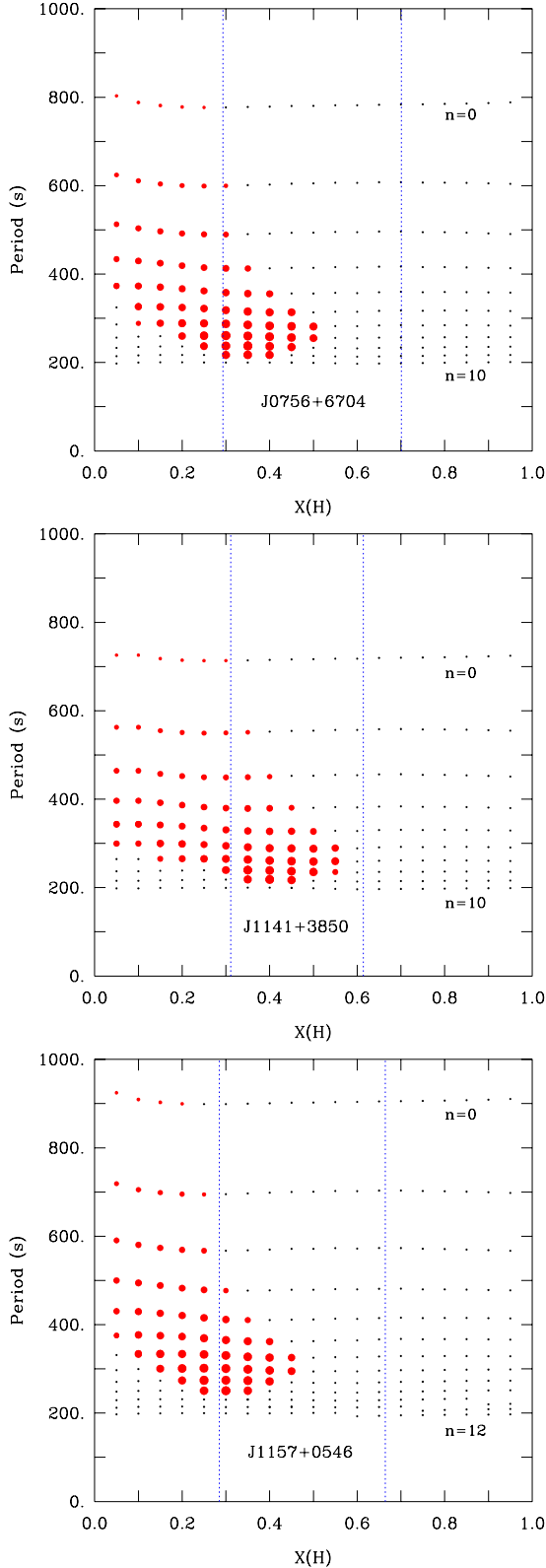


Figure 1. Period spectrum for radial modes as a function of envelope composition for models of J0756 (top), J1141 (middle), and J1157 (bottom). Excited modes are shown as red dots while the black dots denote stable modes. The size of the red dots provides a logarithmic measure of the imaginary part of the eigenfrequency: larger dots correspond to more unstable modes. The blue lines indicate the range in composition based on the $1\text{-}\sigma$ uncertainties of the He abundance measured from the optical spectra.

gating the stability problem – specified by the fixed values of the effective temperature, surface gravity, mass, and a variable value of the envelope composition (a varying mixture of H and He). Mode driving, if any, is associated only with the partial ionization of H and He as these models assume $Z = 0$. Some of our results are depicted in Figure 1, where we show the behavior of the spectrum of excited p -modes (with $\ell = 0$ in this specific example) as a function of the mass fraction of H in the envelope. In all three cases, we find H/He mixtures that could potentially lead to pulsations with 200 – 800 s periods. None of the g -modes investigated (extending in period up to 10,000 s) were found to be excited in our models. In addition, no excitation – p - or g -mode – was found in similar models for the three other spectroscopic targets initially considered (i.e. J0751–0141, J1238+1946, and J1625+3632).

The dotted blue lines correspond to the $1\text{-}\sigma$ uncertainties on the He abundance in the photosphere of each pre-ELM WD. Whether the He is a product of a recent shell flash or has not yet settled out of the atmosphere following the formation of the WD, it is reasonable to assume that the He abundance increases as a function of depth in the star and could thus be higher in the driving region. This would effectively move the dotted blue lines to the left and make our models more unstable to pulsations.

3. OBSERVATIONS

We obtained timeseries photometry of J0756+6704 ($g = 16.38$ mag; hereafter J0756) using the Smithsonian Astrophysical Observatory’s 1.2 m telescope at the Fred Lawrence Whipple Observatory equipped with KeplerCam (Szentgyorgyi et al. 2005) on 2016 January 16. We obtained 282×30 s exposures over 4.2 hr. The chip was binned 2×2 yielding a ≈ 22 s overhead per exposure and a plate scale of 0.67 arcsec pixel $^{-1}$. Observations were obtained using an SDSS- g filter under mixed conditions with a median seeing of ≈ 2.7 arcsec.

We obtained timeseries photometry of J1141+3850 ($g = 19.06$ mag) and J1157+0546 ($g = 19.82$ mag) (hereafter J1141 and J1157, respectively) using the 8 m Gemini-North telescope with the Gemini Multi-Object Spectrograph (GMOS, Hook et al. 2004) on 2016 February 17 as part of the queue program GN-2016A-Q-59. To reduce the read-out time and the telescope overhead to ≈ 15 s, we binned the chip by 4×4 , resulting in a plate scale of 0.29 arcsec pixel $^{-1}$. We obtained 289×10 s exposures over 2 hr for J1141 and 207×20 s exposures over 2 hr for J1157. In both cases, observations were obtained using an SDSS- g filter. Conditions were photometric with a median seeing of ≈ 0.7 arcsec.

For reductions and calibrations we use the standard Image Reduction and Analysis Facility (IRAF) routines and Gemini GMOS routines under IRAF coupled with the daily bias and twilight sky frames. For J0756 (J1141 and J1157), we identify 22 (7, 4) non-variable reference stars that are on the same CCD and amplifier as the target and use them to calibrate the differential photometry.

4. PHOTOMETRIC ANALYSIS

We used the PERIOD04 package (Lenz & Breger 2005) to compute Fourier transforms (FTs) from the light curves of all three targets and extracted the significant pulsation frequencies. Pulsation frequencies are taken as significant if the amplitude exceeds $4\langle A \rangle$ where $\langle A \rangle$ is the mean amplitude of the FT from 0 to the Nyquist frequency.

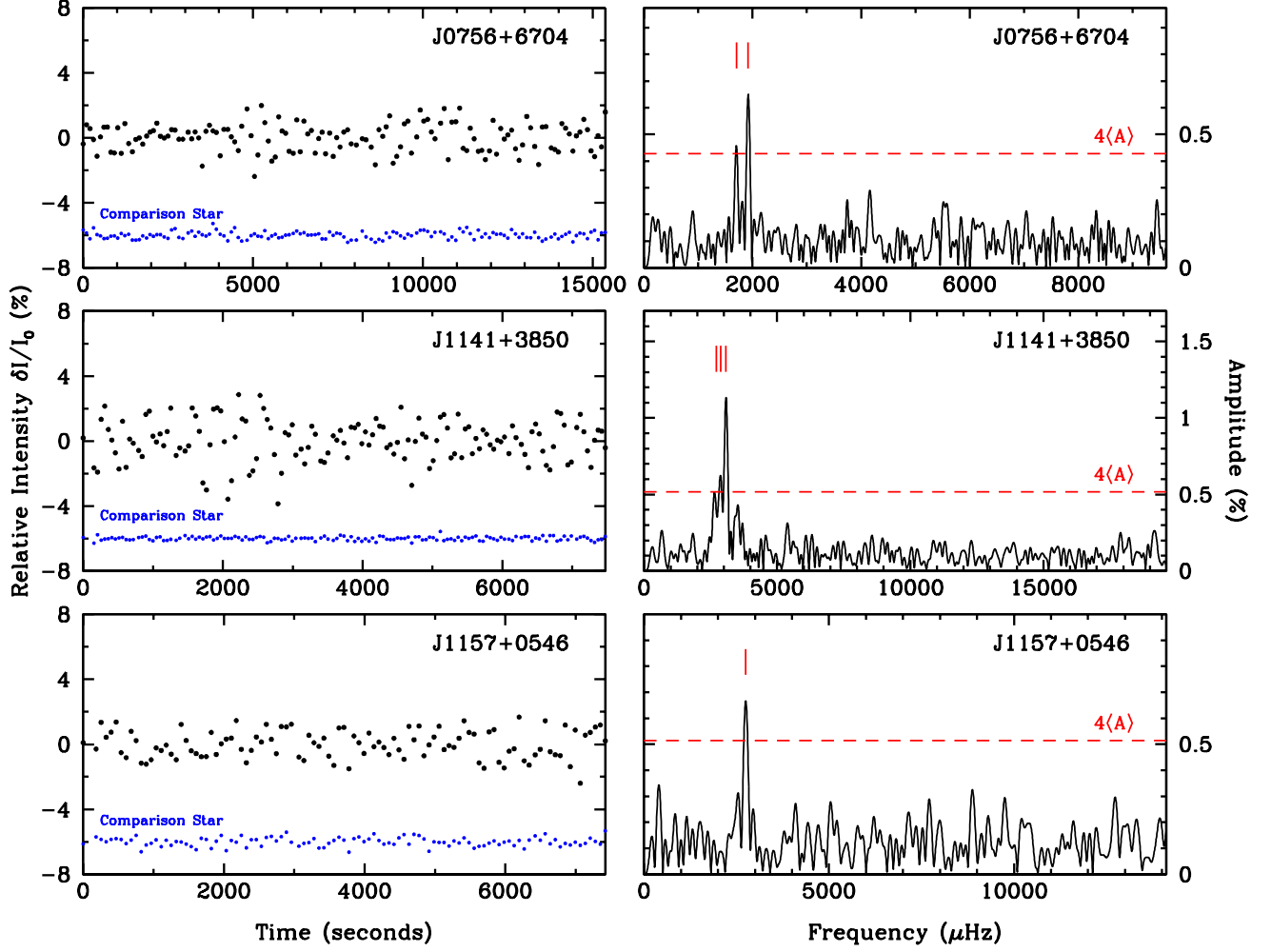


Figure 2. Left: observed light curves (black dots) for the three new pulsating pre-ELM WDs where a two-point boxcar smoothing has been applied. We also plot, in blue, the light curve of the brightest comparison star in the field, offset by -6% for clarity. Right: Fourier amplitude spectra of the observed light curves. The bandpass is plotted from 0 to the Nyquist frequency. We mark the $4\langle A \rangle$ significance level as a dashed red line. The red tick marks denote the location of the significant frequencies.

In Figure 2 we plot the discovery light curves for the three new pulsating ELM WDs and also include the brightest comparison star in the field for reference. We also display the FT for each pulsator and identify the significant peaks in each case.

Table 1 summarizes the detected modes listing the period, frequency, and relative amplitude. We also include the signal-to-noise ratio (S/N) of each signal, calculated by comparing the mode amplitude to the average FT amplitude after subtracting out the significant periods of variability.

4.1. J0756+6704

J0756 is a $T_{\text{eff}} = 11640 \pm 250$ K, $\log g = 4.90 \pm 0.14$ pre-ELM WD with $\log(\text{He}/\text{H}) = -0.60 \pm 0.38$, $M = 0.181 \pm 0.011 M_{\odot}$ at a distance of 1.6 ± 0.3 kpc⁴ (Gianninas et al. 2015). It is found in a 0.61871 days orbit with a companion that has a minimum mass of $0.82 \pm 0.03 M_{\odot}$. The top panels of Figure 2 show the Kepler-

Cam light curve and FT for J0756. We detect two significant periods in J0756 at 521 and 587 s with relative amplitudes of 0.64% and 0.43%, respectively. These periods are somewhat longer than predicted by the models depicted in Figure 1.

A preliminary exploration of a grid of appropriate pulsation models is able to reproduce the two observed periods in J0756. The chosen model has $T_{\text{eff}} = 11619$ K, $\log g = 4.86$, an envelope composition of $X(\text{H}) = 0.395$, an envelope mass of $\log M_{\text{H}}/M_{\star} = -1.87$, and assumes a convective efficiency of $\text{ML2}/\alpha = 1.0$ (Van Grootel et al. 2013), a total mass of $0.186 M_{\odot}$ and a core of pure He.

The model reproduces the observed periods almost exactly with the 521 s period attributed to an $\ell = 0, k = 2$ mode and the 587 s period corresponding to an $\ell = 2, k = 0$ mode. Both of these are p -modes; the former is a radial mode while the latter is a non-radial mode. However, this solution is not unique; we currently have two detected periods to work with and these provide only modest constraints on the models. Nonetheless, these periods are consistent with those predicted by the model depicted in Figure 1, albeit for the lowest value of $X(\text{H})$ within the $1\text{-}\sigma$ range.

⁴ Distance and mass estimates are based on the evolutionary models of Althaus et al. (2013); Istrate et al. (2014) models yield estimates that differ by less than 5% (Gianninas et al. 2015).

Table 1
Photometric Parameters for the New Pulsating ELM WDs

SDSS	Period (s)	Frequency (μHz)	Amplitude (%)	S/N
J0756+6704	521 ± 1	1921 ± 4	0.64 ± 0.08	6.6
	587 ± 2	1705 ± 6	0.43 ± 0.08	4.4
J1141+3850	325 ± 1	3073 ± 7	1.12 ± 0.10	9.8
	346 ± 2	2886 ± 14	0.56 ± 0.10	4.9
	368 ± 2	2719 ± 16	0.51 ± 0.09	4.5
J1157+0546	364 ± 1	2751 ± 11	0.66 ± 0.10	5.5

4.2. J1141+3850

J1141 is a $T_{\text{eff}} = 11290 \pm 210$ K, $\log g = 4.94 \pm 0.10$ pre-ELM WD with $\log(\text{He}/\text{H}) = -0.53 \pm 0.27$, $M = 0.177 \pm 0.011 M_{\odot}$ at a distance of 5.2 ± 0.8 kpc (Gianninas et al. 2014a). It is found in a 0.25958 days orbit with a companion that has a minimum mass of $0.765 \pm 0.04 M_{\odot}$. The middle panels of Figure 2 show the GMOS light curve and FT for J0756. In this case, we detect three significant modes with periods of 325, 346, and 368 s and relative amplitudes of 1.12, 0.56 and 0.51%, respectively. Overall, the three significant periods are shorter and have larger relative amplitudes than the modes observed in J0756.

Of potential interest in the case of J1141 is the spacing of the observed pulsation modes. The frequency spacings separating the three modes are $187 \pm 16 \mu\text{Hz}$ and $167 \pm 21 \mu\text{Hz}$, which agree within the uncertainties. If these spacings are in fact equal, then it is possible that we are observing a triplet produced by the rotational splitting of an $\ell = 1$ mode. If we assume this is correct, we can estimate the rotation period of J1141. Taking a weighted mean of the two spacings yields an average spacing of $178 \pm 13 \mu\text{Hz}$ which corresponds to a relatively short rotational period of 1.6 ± 0.1 hr.

We stress that rotational splitting is only one potential explanation for the observed periods. It is more likely that we have detected p -mode periodicities with different values of the degree ℓ . Indeed, the spacings between consecutive periods are too small for all three modes to belong to the same degree value. On the other hand, the period difference of 43 s between the two extreme values is comparable to what theory suggests in that period range for two adjacent modes with the same ℓ value, i.e., ~ 40 s. This would also account for the difference between the middle period of 346 s and the possible period of 384 s, both of them belonging to a different value of ℓ than the pair 325-368 s.

4.3. J1157+0546

J1157 is a $T_{\text{eff}} = 11870 \pm 260$ K, $\log g = 4.81 \pm 0.13$ pre-ELM WD with $\log(\text{He}/\text{H}) = -0.55 \pm 0.35$, $M = 0.186 \pm 0.011 M_{\odot}$ at a distance of 9.2 ± 1.9 kpc (Gianninas et al. 2014a). It is found in a 0.56500 days orbit with a companion that has a minimum mass of $0.46 \pm 0.05 M_{\odot}$. The bottom panels of Figure 2 show the GMOS light curve and FT for J1157. We detect a single significant periodicity at 364 s with a relative amplitude of 0.66 %. This is perfectly consistent with the predictions of

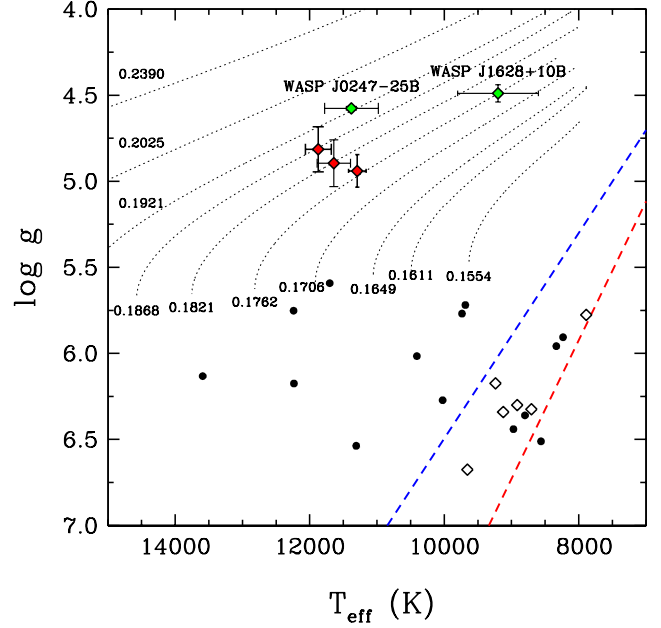


Figure 3. Region of the $T_{\text{eff}}\text{--}\log g$ plane containing the instability strip of pulsating ELM WDs (lower left), six of the known ELM pulsators (white diamonds), and ELM WDs where no pulsations are detected (black dots). The red diamonds represent the three new pulsators from this paper. The green diamonds correspond to the pulsators in EL CVn-type systems. The dashed lines denote the empirical blue and red boundaries of the instability strip (Gianninas et al. 2015; Tremblay et al. 2015). The dotted black lines represent the evolutionary tracks for He-core ELM WDs from Althaus et al. (2013) with stars evolving from the upper right to the lower left. The individual tracks are labeled by the final mass in M_{\odot} .

the models shown in Figure 1. However, given that only a single period is detected in J1157, it is impossible to draw any detailed conclusions with regards to the exact pulsation mode that is observed.

5. DISCUSSION

5.1. Three New Pulsating Pre-ELM WDs

The discovery of these three new pulsating, mixed-atmosphere, pre-ELM WDs represents yet another success of the predictive power of non-adiabatic pulsation theory. In Figure 3 we plot the location of the three new pulsators in the $T_{\text{eff}}\text{--}\log g$ plane along with the previously known ELM WD pulsators which lie within the confines of the extended ZZ Ceti instability strip. Given the remarkable similarities in the atmospheric parameters of all three targets, it could appear at first glance as if these pre-ELM WDs form an entirely new class of pulsators.

Those stars are certainly different from the more compact pulsating ELM WDs found in the ZZ Ceti instability strip illustrated in Figure 3. First, they are p -mode pulsators whereas the latter are all g -mode variables with much longer periods⁵. Second, the driving process in the three objects described here is dominated by the usual κ -mechanism—with some contribution from convective driving—whereas the ZZ Ceti ELMs are excited by convective driving at the base of a pure H ionization zone. Third, the three stars of interest have mixed H/He atmosphere-envelope compositions—the pres-

⁵ A possible detection of a p -mode was reported by Hermes et al. (2013b) in J1112+1117, but the evidence is marginal and has not been confirmed.

ence of He playing a critical role in the driving process—whereas the ZZ Ceti ELMs are excited by a mechanism that occurs in pure H layers.

On the other hand, the three new pulsators bear a strong similarity with the other currently known pre-ELM WD pulsators found in the EL CVn-type binaries WASP J2047–25B and WASP J1628+10B (Maxted et al. 2013, 2014b). The latter are also p -mode variables with periods in the same range as those reported here and they occupy the same general region in the spectroscopic Hertzsprung–Russell diagram, i.e., on the contracting branches of the evolutionary tracks (see Figure 3). Indeed, there is a significant difference in the mean densities of the new pre-ELM pulsators versus the pulsators in the EL CVn systems. Based on our estimates of the mass and radius of the pre-ELM WD pulsators from the Althaus et al. (2013) models, we calculate mean densities of $\approx 16, 19, 12 \text{ g/cm}^3$ for J0756, J1141, and J1157, respectively. In contrast, the mean density for WASP J2047–25B and WASP J1628+10B is $\approx 5 \text{ g/cm}^3$. In addition, the companions in the EL CVn systems are well-constrained through the observed eclipses and that they are double-lined systems. It is clear that for both WASP systems the companions are main sequence A stars. In contrast, the pre-ELM WD binaries are all single-lined systems where the unseen companion is assumed to be a cooler, more massive WD.

Because the spectra of the pulsating pre-ELM WD components in the EL CVn systems are heavily polluted by the light of the A-star companions, it has been difficult to infer their atmospheric He abundance; this important quantity is still not available. If these objects belong to the same class of pulsators as the three pre-ELM WDs reported in this paper, He must necessarily be present in substantial quantity in the atmospheres of the pre-ELM WD components of the EL CVn systems. According to this scheme, the He content in WASP J2047–25B should be roughly comparable to the values we need for explaining the existence of the three pulsators discussed here, while it should be significantly lower (by perhaps a factor of 2 by mass fraction) in the cooler WASP J1628+10B which would be part of a different instability strip than the former. This situation is analogous to the continuum of instability strips discussed by Van Grootel et al. (2015) in the context of mixed H/He atmosphere WDs of the GW Lib type.

5.2. The Origin of Helium in Pre-ELM WDs

Helium is the key ingredient that allows J0756, J1141, and J1157, as well as the two WASP pulsators, to be unstable to pulsations. Consequently, understanding why the He is present, and in such significant quantity is fundamental if we are to explain why these unique pre-ELM WDs exist.

The evolutionary sequences of Althaus et al. (2013) and Istrate et al. (2014) predict that ELM WDs within a certain mass range will experience one or more H shell flashes as they evolve. Indeed, Gianninas et al. (2014a,b) suggested that the observed He and metals such as Ca were possibly the result of a recent shell flash. The shell flash produces He and could also mix up the interior of the star sufficiently to bring metals back to the surface. However, the masses inferred for the three new pulsating pre-ELM WDs are below the mass threshold for which shell flashes are expected. This is particularly true for the Istrate et al. (2014) models, which require $M > 0.21 M_\odot$ for shell flashes to occur.

If shell flashes are not the source of the He, then it is likely

that the He in these particular pre-ELM WDs is simply left over from the formation of the WD itself and has not completely diffused out of the atmosphere yet. If this scenario is correct, then our estimate of the H layer mass is particularly useful. Our preliminary estimate of $\log M_{\text{H}}/M_\star = -1.87$ for J0756 implies a relatively thick surface H layer, which is consistent with the evolutionary models of Althaus et al. (2013) and Córscico et al. (2016).

5.3. Future Prospects

Extensive follow-up observations of these new mixed-atmosphere, pulsating pre-ELM WDs will be useful in identifying all of their periodicities. As J0756 is the brightest of the three targets, it is well-suited for an extended observing campaign. Simultaneous multicolor photometry in three or more bands would be particularly useful for proper mode identification as the relationship between pulsation amplitude and wavelength is directly related to the ℓ value of the observed mode. A detailed asteroseismic analysis of such observations would help constrain the internal structure of these pre-ELM WDs. As our preliminary analysis portends, the mass of H at the surface could be constrained and lead to improved evolutionary models.

A.G. and M.K. gratefully acknowledge the support of the NSF under grant AST-1312678, and NASA under grant NNX14AF65G. This work was supported in part by the Natural Sciences and Engineering Research Council of Canada. G.F. also acknowledges the contribution of the Canada Research Chair Program. This work was supported in part by the Smithsonian Institution.

Facilities: Gemini (GMOS), FLWO: 1.2m (KeplerCam)

REFERENCES

- Althaus, L. G., Miller Bertolami, M. M., & Córscico, A. H. 2013, *A&A*, 557, A19
- Bell, K. J., Kepler, S. O., Montgomery, M. H., et al. 2015, in *ASP Conf. Ser.* 493, 19th European Workshop on White Dwarfs, ed. P. Dufour, P. Bergeron, & G. Fontaine (San Francisco, CA: ASP), 217
- Brassard, P., Pelletier, C., Fontaine, G., & Wesemael, F. 1992, *ApJS*, 80, 725
- Brown, W. R., Gianninas, A., Kilic, M., Kenyon, S. J., & Allende Prieto, C. 2016, *ApJ*, 818, 155
- Córscico, A. H., & Althaus, L. G. 2014, *A&A*, 569, A106
- . 2016, *A&A*, 585, A1
- Córscico, A. H., Althaus, L. G., Serenelli, A. M., et al. 2016, *A&A*, 588, A74
- Fontaine, G., & Brassard, P. 2008, *PASP*, 120, 1043
- Fontaine, G., Brassard, P., Wesemael, F., & Tassoul, M. 1994, *ApJL*, 428, L61
- Gianninas, A., Bergeron, P., & Ruiz, M. T. 2011, *ApJ*, 743, 138
- Gianninas, A., Dufour, P., Kilic, M., et al. 2014a, *ApJ*, 794, 35
- Gianninas, A., Hermes, J. J., Brown, W. R., et al. 2014b, *ApJ*, 781, 104
- Gianninas, A., Kilic, M., Brown, W. R., Canton, P., & Kenyon, S. J. 2015, *ApJ*, 812, 167
- Hermes, J. J., Montgomery, M. H., Gianninas, A., et al. 2013a, *MNRAS*, 436, 3573
- Hermes, J. J., Montgomery, M. H., Winget, D. E., et al. 2012, *ApJL*, 750, L28
- Hermes, J. J., Montgomery, M. H., Winget, D. E., et al. 2013b, *ApJ*, 765, 102
- Hook, I. M., Jørgensen, I., Allington-Smith, J. R., et al. 2004, *PASP*, 116, 425
- Istrate, A. G., Tauris, T. M., Langer, N., & Antoniadis, J. 2014, *A&A*, 571, L3
- Jeffery, C. S., & Saio, H. 2013, *MNRAS*, 435, 885
- Jeffery, C. S., & Saio, H. 2016, *MNRAS*, 458, 1352
- Kilic, M., Hermes, J. J., Gianninas, A., & Brown, W. R. 2015, *MNRAS*, 446, L26
- Lenz, P., & Breger, M. 2005, *CoAst*, 146, 53
- Maxted, P. F. L., Serenelli, A. M., Marsh, T. R., et al. 2014a, *MNRAS*, 444, 208
- Maxted, P. F. L., Serenelli, A. M., Miglio, A., et al. 2013, *Natur*, 498, 463
- Maxted, P. F. L., Bloemen, S., Heber, U., et al. 2014b, *MNRAS*, 437, 1681

Szentgyorgyi, A. H., Geary, J. G., Latham, D. W., et al. 2005, BAAS, 37,
1339
Tremblay, P.-E., Gianninas, A., Kilic, M., et al. 2015, ApJ, 809, 148

Van Grootel, V., Fontaine, G., Brassard, P., & Dupret, M.-A. 2013, ApJ, 762,
57
—, 2015, A&A, 575, A125
Winget, D. E., & Kepler, S. O. 2008, ARA&A, 46, 157